Science of Sintering, **53** (2021) 535-548

https://doi.org/10.2298/SOS2104535J

UDK: 663.97.051.8; 543.4

The Influence of pH on Electrochemical Behavior of Nicotine-Clay based Electrodes

Nataša Jović-Jovičić[*)], Tihana Mudrinić, Aleksandra Milutinović-Nikolić, Predrag Banković, Zorica Mojović

University of Belgrade – Institute of Chemistry, Technology and Metallurgy, Department of Catalysis and Chemical Engineering, Njegoševa 12, Belgrade, R. Serbia

Abstract:

Montmorillonite based clay was acid activated. Nicotine was adsorbed on untreated and acid activated clay from its aqueous solution at either pH=6 or pH=9.26 (unadjusted pH solution). The XRD analysis revealed that the 001 basal spacing of montmorillonite after nicotine adsorption was around 1.38 nm, regardless of clay treatment or pH of adsorption. The obtained values for basal spacing indicate that nicotine is in monolayer arrangement. In order to investigate electrochemical properties, untreated and acid activated clay, with and without nicotine, were used as modifier of carbon paste electrode. Cyclic voltammetry and electrochemical impedance spectroscopy were employed to study electrochemical response of clay-modified electrodes toward ferrocyanide probe. The nicotine-modified untreated clay used as paste electrode showed enhanced electrochemical response toward ferrocyanide probe in comparison to electrode based on clay without nicotine. On the other hand, adsorbed nicotine on acid activate clay resulted in lower electrode activity. Electrochemical response of adsorbed nicotine was studied at different pH. Nicotine oxidation at each of investigated samples followed the same trend regardless of clay treatment or pH at which adsorption was performed. For all samples, nicotine oxidation peak potential showed linear dependence on pH in pH range from 3.7 to 9.0, with slopes close to the value of 59 $mVdec^{-1}$ expected for equal number of protons and electrons involved in the reaction. The nicotine reduction process was best resolved at pH = 1 at potential around -1.35 V, while the following cathodic wave observed at potential around -1.5 V was ascribed to the cathodic hydrogen reduction. Mechanism of electrochemical oxidation was not influenced by pH of adsorption, i.e., nicotine form. The amount of adsorbed nicotine was not correlated with the electrochemical activity suggesting that only small number of adsorbed nicotine was involved in electrochemical response.

Keywords*: Nicotine; Montmorillonite; Cyclic voltammetry; Electrochemical impedance spectroscopy; Ferrocyanide probe.*

1. Introduction

Clay minerals have been investigated for over several decades but their possible applications are still intensely researched in various areas: as precursors for porous ceramics [1], adsorbents for anion removal [2], catalyst supports [3], greenhouse gas control [4]. One of interesting application of clays is in development of electrode materials. Aluminosilicate-

[*)] **Corresponding author:** natasha@nanosys.ihtm.bg.ac.rs

modified electrodes have found numerous applications for electroanalytical applications [5] as photoelectrocatalyst [6] or electrocatalyst [7,8]. The properties of clays such as ion-exchange properties, chemical stability, layered aluminosilicate structure and low cost made them desirable material. The simple procedures such as acid activation, pillaring or modification with organic substances [9] easily broaden the range of clay properties and their possible applications.

Organically modified clay (organoclay) is inorganic-organic composite material consisting of clay, as inorganic part, and some organic substance. Several methods can be employed for synthesis of these composites [10]. Organoclay-based composite electrodes have shown to be efficient sensors for various analytes [11].

In our previous publication [12] the nicotine adsorption was tested on standard Wyoming (SWy-2) montmorillonite and acid-modified sample and the optimal pH values for nicotine adsorption were determined.

Nicotine ($C_{10}H_{14}N_2$) is a nitrogen alkaloid present in concentrations as high as 3% in the dried leaves of the tobacco plant (*Nicotiana tabacum*). Nicotine is soluble in both water and hydrophobic solvents and has two basic nitrogen atoms, in pyridine and pyrrolidine ring, with pKa_1=3.04 and pKa_2 =7.84, respectively. Nicotine is the highly toxic substance. It was suggested that human lethal dose is within interval from 0.5 to 1.0 mg kg^{-1}, corresponding to the total lethal dose of 30-60 mg consumed at once for adults [13]. During the manufacturing of tobacco nicotine is released into the environment. The wastewaters from this industry containing nicotine are released to public wastewater facilities or even directly to natural aquatic recipients. Tobacco dust is used as addition to compost or as filler in fertilizers [14]. Therefore, the presence of nicotine in environment is recognized as one of significant problems by US Environmental Protection Agency [15]. Bearing this in mind, the possibility of using electrochemical methods in nicotine detection can be regarded as promising task.

In this paper clays with adsorbed nicotine were used as modifiers of carbon paste electrode. In the first part of investigation, the electroactivity of such electrodes toward ferrocyanide probe were tested. In the second part, the electrochemical activity of nicotine adsorbed at different pH was investigated. The aim of the work was to correlate, if possible, adsorptive and electrochemical properties.

2. Materials and Experimental Procedures

Nicotine ((S)-3-(1-Methyl-2-pyrrolidinyl) pyridine) was obtained from Alfa – Aesar Chemical Company with a chemical purity of 99 %.

Starting clay was purchased from The Source Clays Repository - The Clay Minerals Society, from New Castle formation, Crook County, Wyoming, SAD (MW). According to Safety Data Sheet [16] it consists of clay mineral montmorillonite (90-100 %) and quartz (5-10 %). The specific gravity of approx. 2.2 gcm^{-3} and the cation exchange capacity of 74.4 mmol monovalent cation per 100 g of dry clay are given. The chemical composition (mass%) of the sample was estimated by Mermut and Cano, 2001 [17]: SiO_2 – 61.46±1.29; Al_2O_3 – 22.05±0.19; Fe_2O_3 – 4.37±0.06; MgO – 2.94±0.02; CaO - 1.18±0.03; Na_2O – 1.47±0.03; K_2O – 0.20±0.01 and TiO_2 – 0.09±0.00.

Acid modification was performed by constant stirring (120 rpm) of MW with 4.5M HCl during 2 h at 90°C, with solid to liquid ratio 1:4.5 [18]. The dispersion was transferred into a dialysis bag filled with deionized water (12 MΩ). Deionized water was continually changed until the dialysate was free of chloride (confirmed by precipitation test with $AgNO_3$). Finally, the solid phase was dried at 110°C and denoted as MWA.

The adsorption of nicotine (C_0=0.75 mmol dm^{-3}, V=50.00 cm^3) onto MW and MWA (m_{ads}=50 mg) was performed in a batch system at 25ºC in thermostated shaker (Memmert WNE 14 and SV 1422). Thermo Electron Nicolet Evolution 500 UV-Vis was used for

monitoring the nicotine concentration before and after adsorption (λ_{max}=261 nm). A PHM240 MeterLab® pH meter was used to control the pH of solution. The adsorption was performed on two characteristic pH values, i.e., 6 and 9.26 (unadjusted pH value) [12].

The amount of adsorbed nicotine at equilibrium time was calculated using equation:

$$q_e = \frac{(C_0 - C_e)\cdot V}{m_{ads}} \qquad (1)$$

where C_0 and C_e are initial and equilibrium nicotine concentration (mmol dm^{-3}), V is volume of nicotine solution (cm^3) and m_{ads} is mass of adsorbent (mg). The samples were denoted in accordance to the applied clay and starting pH, rounded to an integer (MW6, MW9, MWA6, MWA9).

The effect of the acid modification and nicotine adsorption on montmorillonite structure was tested using Rigaku SmartLab automatic multipurpose X-ray diffractometer with Cu anode (λ=0.1542 nm). The instrument was equipped with low background Si sample holder support and 1D D/teX 250 Ultra detector in XRF mode. The 2θ range from 2° to 50°, with the scanning rate of 3.0° min^{-1} was applied.

The materials with adsorbed nicotine were used as modifiers of carbon paste electrode. In order to use the clay samples as electrode material carbon paste electrode (CPE) with investigated adsorbent/adsorbate systems were prepared. Porous material/carbon paste was prepared by hand mixing of clay and carbon black Vulcan XC72 (Cabot Corp.) in ratio 1:2 with paraffin oil. The resulting pastes were packed into the hollow (1 mm diameter) Teflon tube and the electrical contact was provided by a copper wire and used as working electrode. Clay/carbon paste electrodes were designated in the same manner as the clay samples.

The electrochemical measurements were performed using Autolab electrochemical workstation (Autolab PGSTAT302N, Metrohm-Autolab BV, Netherlands). The reference electrode was Ag/AgCl in 3 M KCl, a platinum rod served as a counter electrode, while modified CPE served as working electrode. Impedance measurements were carried out at open circuit potential (OCP) using a 5 mV rms sinusoidal modulation in the 10 kHz-10 MHz frequency range. The 1 mM $K_4[Fe(CN)_6]$ in 0.2 M KCl was used as electrolyte. Cyclic voltammetry was performed at scan rate of 20 mVs^{-1} in the same electrolyte. The response of the modified CPE toward $K_4[Fe(CN)_6]$ was tested at different pH values by cyclic voltammetry at scan rate of 100 mVs^{-1}.

Solutions with different pH values were prepared using various solutions: 0.1 M hydrochloric acid for pH=1.0; 0.1 M acetate buffer for pH 3.7 and 4.9; 0.1 M phosphate buffer for pH 6.9 and 7,7; 0.1 M carbonate/bicarbonate buffer for pH 9.0 and 10.2 and 0.1 M NaOH for pH=13. Buffers were freshly made, measured using PHM240 MeterLab® pH meter and saturated with nitrogen prior to addition of $K_4[Fe(CN)_6]$.

The nicotine desorption study was carried out in thermostatic shaker at 25 ^{0}C. Prior to desorption, the samples MW and MWA were saturated with nicotine in adsorption process on pH=6 and 9.26. The 50.0 mg of nicotine-saturated sample (MW6, MW9, MWA6, MWA9) was dispersed in 25.00 mL of 0.1 mol dm^{-3} HCl in a conical flask. The desorption was monitored after 30 minutes. After each desorption process, the liquid phase was separated by centrifugation on 17000 rpm during 6 min, and nicotine concentration analyzed at 261 nm using Thermo Electron Nicolet Evolution 500 UV–VIS spectrophotometer. The percent of retained nicotine after desorption in predeterminate times was calculated according to equation:

$$\%Ret = \frac{n_{ads} - n_{des}}{n_{ads}} \cdot 100\% \qquad (2)$$

where n_{ads} is amount of nicotine adsorbed after equilibrium time (saturation) and n_{des} is the amount of desorbed nicotine.

3. Results and Discussion

3.1. Adsorption test

The selected clay samples were saturated by nicotine in adsorption process. The adsorption of nicotine was pH dependent with maximum at pH = 6 and pH = 9 for MW and MWA, respectively [12]. The amount of adsorbed nicotine after equilibrium time of 180 min was 0.4335 mmol g^{-1}, 0.3231 mmol g^{-1}, 0.3825 mmol g^{-1}, and 0.5413 mmol g^{-1} for MW6, MWA6, MW9 and MWA9, respectively.

3.2. XRD

The results of XRD analysis for MW and MWA, together with corresponded samples after nicotine adsorption on pH = 6 and 9 (MW6, MW9, MWA6, MWA9) are shown at Fig. 1a and 1b.

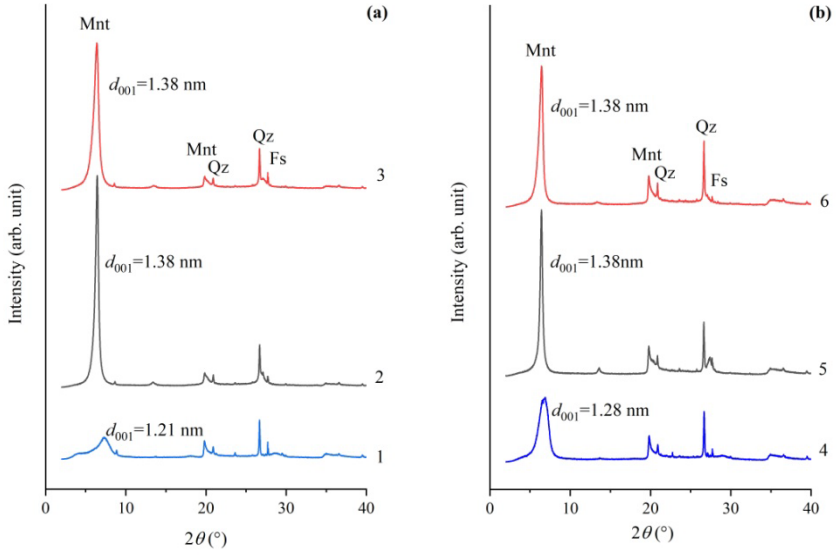

Fig. 1. The XRD spectra of (1) – MW, (2) – MW6; (3) – MW9; (4) – MWA; (5) – MWA6; (6) – MWA9; where Mnt –montmorillonite, Qz – quartz, and Fs – feldspar.

According to the X-ray powder diffraction results (Fig. 1) the following phases were identified in the investigated samples: montmorillonite (Mnt) as the main constituent and quartz (Qz), and feldspar (Fs) as associated minerals [19]. The acid activation resulted in a slight increase of the d_{001} value from 1.21 nm for MW to 1.28 nm for MWA. This increase can be assigned to auto-transformation process that occurs during acid activation process [9].

The 001 basal spacing of both starting samples (MW and MWA) after nicotine adsorption increased to the values around 1.38 nm. This finding was the same for all investigated samples, regardless of pH value applied during adsorption process. Since the referred literature value for montmorillonite lamellae is approx. 0.97 nm [9,20] the increasing of basal space of 0.41 nm can be attributed to intercalated nicotine in the interlamellar space.

According to the literature data, the obtained value of 0.41 nm indicated that nicotine was intercalated in form of monolayer between silicate layers. Rebitski *et al.* [21] found that

basal spacing of intercalated metformin in montmorillonite structure was 1.35 nm, i.e. the thickness of guest molecule was 0.4 nm. The authors suggested that obtained value correspond to monolayer of metformin present in interlamellar region. The similar observation was found by Ruiz-García *et al.* [22] for carbon-montmorillonite materials obtained from intercalated sucrose. The basal spacing after carbonization process was 1.31 nm that corresponds to formation of a monolayer of carbon atoms between the silicate layers.

The results of XRD study indicated that nicotine was intercalated into interlamellar space regardless nicotine form (monoprotonated at pH=6 and molecular at pH = 9.26).

3.3. Electrochemical properties

Carbon paste electrode modified with investigated clay samples were characterized by cyclic voltammetry and electrochemical impedance spectroscopy. Potassium hexacyanoferrate (II) was used as a redox probe. Cyclic voltammograms (CV) recorded for all investigated clay samples exhibited pair of peaks corresponding to the oxidation and the reduction peaks of $[Fe(CN)_6]^{3-/4-}$ couple (Fig. 2a and 2b).

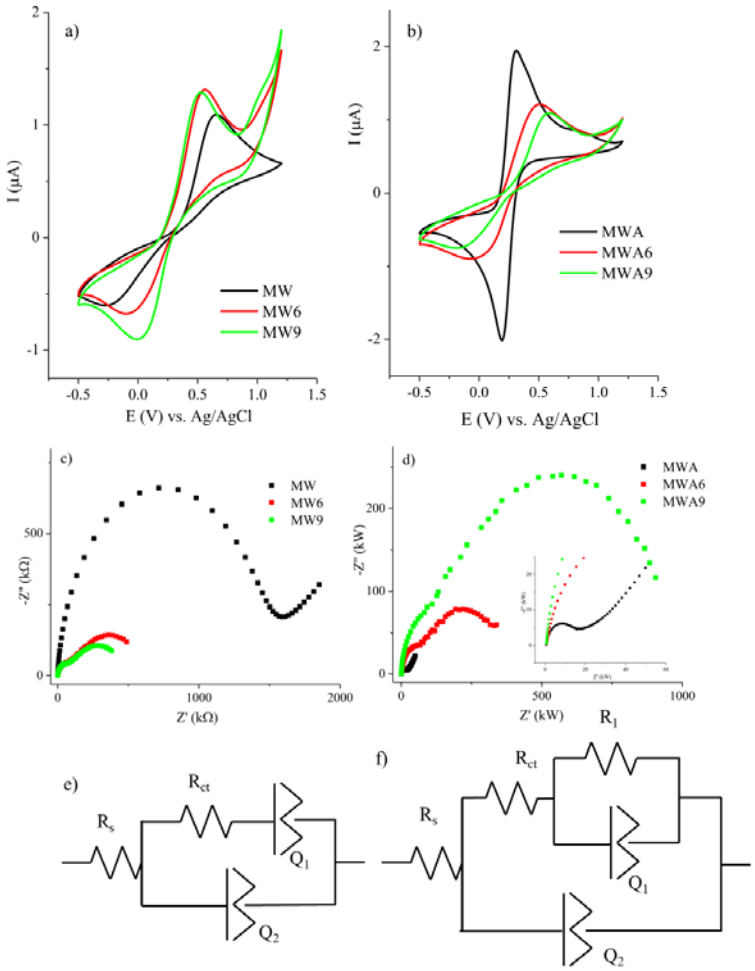

Fig. 2. a) and b) Cyclic voltammograms of electrodes recorded in 1mM $K_4[Fe(CN)_6]^{3-/4-}$+ 0.2 M KCl at scan rate of 20 mV s^{-1}; c) and d) Electrochemical impedance spectra of electrodes recorded at OCP in same solution. Inserted picture in d) enlarged part of EIS spectra for high frequencies; e) and f) Randles equivalent circuit used to fit experimental data.

Half wave potentials ($E_{1/2}$), peak-to-peak separation (ΔE) values and anodic to cathodic current ratio observed for investigated electrodes are presented in Table I.

Tab. I Half-wave potentials ($E_{1/2}$), anodic to cathodic peak separation (ΔE) values and anodic to cathodic current ratio for the oxidation of 1 mM $K_4[Fe(CN)_6]$ in 0.2 M KCl on clay modified CPE.

Sample	ΔE (mV)	$E_{1/2}$ (mV)	I_a (μA)	I_a/I_c
MW	822	224	0.80	2.73
MW6	535	260	0.86	1.58
MW9	466	268	0.84	1.08
MWA	115	250	2.00	0.95
MWA6	442	253	0.97	1.67
MWA9	661	228	0.73	1.77

Acid activated montmorillonite (MW_A) had greater electroactivity than untreated montmorillonite (MW) i.e. lower peak-to-peak separation, higher current, and anodic to cathodic current ratio was close to 1. The observe enhancement can be attributed to the reduced repulsive forces between anionic species and negative layer charge (due to smaller amount of negative layer charge on the acid activated sample [23]).

Addition of nicotine to untreated clay sample led to the increase of current response and lower values of peak-to-peak separation, while the opposite effect was noted for the acid activated sample. It has been already reported [24-26] that introduction of organic species to clay samples led to the enhanced electrochemical response toward $[Fe(CN)_6]^{3-/4-}$. Slightly better electrochemical response toward $[Fe(CN)_6]^{3-/4-}$ was obtained for MW9 than for MW6. The addition of nicotine led to the decrease of electrochemical activity of the acid activated samples. The activity was less affected by cationic form of the adsorbed nicotine than by its neutral form. This effect might be ascribed to the higher amount of the adsorbed nicotine at pH 9 for acid activated sample, particularly for the sites which are essential for enhancement electrochemical response of MW_A toward ferrocyanide probe (i.e. acid sites).

The effective surface area of the investigate electrode was determined using the Randles–Sevcik equation:

$$I_p = 0.4436 \cdot n \cdot F \cdot A \cdot C \cdot \sqrt{\frac{n \cdot F \cdot v \cdot D}{R \cdot T}} \qquad (3)$$

where I_p (A) is the anodic peak current, A (cm^2) is the active surface area of the electrode, C (mol cm^{-3}) is the concentration of $K_4Fe(CN)_6$, F is the Faraday's constant (96,485 C mol^{-1}), R is the universal gas constant (8.314 J mol^{-1} K^{-1}), T is the absolute temperature (298 K), n is the electron transfer number, D ($7.63 \cdot 10^{-6}$ cm^2 s^{-1}) is the diffusion coefficient, and v ($V \cdot s^{-1}$) is the scan rate. The effective surface area was found to be 0.0106 cm^2 (MW), 0.0126 cm^2 (MW6), 0.0121 cm^2 (MW9), 0.0258 cm^2 (MWA), 0.0114 cm^2 (MWA6) and 0.0103 cm^2 (MWA9).

EIS measurements were performed after voltametric experiments, providing electrode saturation with electrolyte and stable value of open circuit potential. The open circuit potential was around 0.2 V for all investigated electrodes. The recorded EIS spectra are presented in Figs. 2c and 2d. Nyquist plots of MW and MW_A consisted of semicircle section at higher frequencies corresponding to charge transfer limiting process and short linear section at lower frequencies corresponding to diffusion-limited process. Nyquist plots of nicotine/clay systems consisted of two semicircles. R_{ct} is determined by kinetically controlled electrochemical reaction of redox probe at the electrode surface.

The modified Randles equivalent circuit (Fig. 2e) was used to fit the obtained spectra for MW and MWA, i.e. CPE modified with clay samples without nicotine.
The circuit consists of internal resistance (R_S) in series with the parallel combination of the constant phase element (Q_2) representing double-layer capacitance and an impedance of a faradaic reaction (serial combination of charge transfer resistance (R_{ct}) and constant phase element (Q_1) representing diffusion). The constant phase element represents non-ideal capacitor with the impedance given as:

$$Z = \frac{1}{Y} = \frac{1}{(i\omega)^n Q} \qquad (4)$$

where Y is the admittance, i is the imaginary unit, ω is the angular frequency, n is the exponent which is associated with the system inhomogeneity and Q has the numerical value of the admittance (1/ |Z|) at ω =1 rad/s.
The constant phase element was introduced instead the double-layer capacitance and Warburg impedance present in original Randles circuit in order to obtain better fitting results. The spectra obtained for CPE modified with clay with adsorbed nicotine were fitted with the circuit presented in Fig. 2f. Low frequency double layer relaxation is described with R_1/Q_1 parallel combination in series with R_{ct}.

The results obtained using fitting with appropriate circuits (2e or 2f) are presented in Table II.

Tab. II The electrochemical parameters obtained by fitting EIS data recorded using electrodes in 1 mM $K_4[Fe(CN)_6]$+ 0.2 M KCl.

Sample	R_{ct} (kΩ)	R_1 (kΩ)	Y_1 (μSs^{n1})	n1	Y_2 (nSs^{n2})	n2
MW	1400	-	2.2	0.4	6.0	0.9
MW6	103	519	1.2	0.6	53.7	0.8
MW9	93	374	1.5	0.6	53.0	0.9
MWA	11	-	27.4	0.3	40.8	0.9
MWA6	70	321	1.2	0.6	29.9	0.8
MWA9	116	899	0.3	0.6	11.7	0.9

Acid activation significantly lowered the value of charge transfer resistance R_{ct}. The lowest charge transfer resistance was obtained MWA electrode, which is in agreement with the activity of this electrode obtained by cyclic voltammetry. The introduction of nicotine to untreated and acid activated sample led to the opposite effects. The charge transfer resistance was significantly lowered for MW6 and MW9 in comparison to starting MW sample. Tonle et. al. [24] noted beneficial effect of incorporation of organic compounds in smectite ascribing this effect to the accumulation of the negatively-charged probes by the positively-charged guest species.
The introduction of nicotine to the acid activated clay sample significantly increased charge transfer resistance. This result might indicate different adsorption sites available in untreated and acid activated samples, or the lower performance of introduced nicotine in comparison to protons.

3.4. Behavior at different pH

Further investigation of the clay samples with adsorbed nicotine was performed by cyclic voltammetry at different pH (Fig. 3). Cyclic voltammograms of the untreated clay and acid activated clay were also recorded for the comparison purpose.

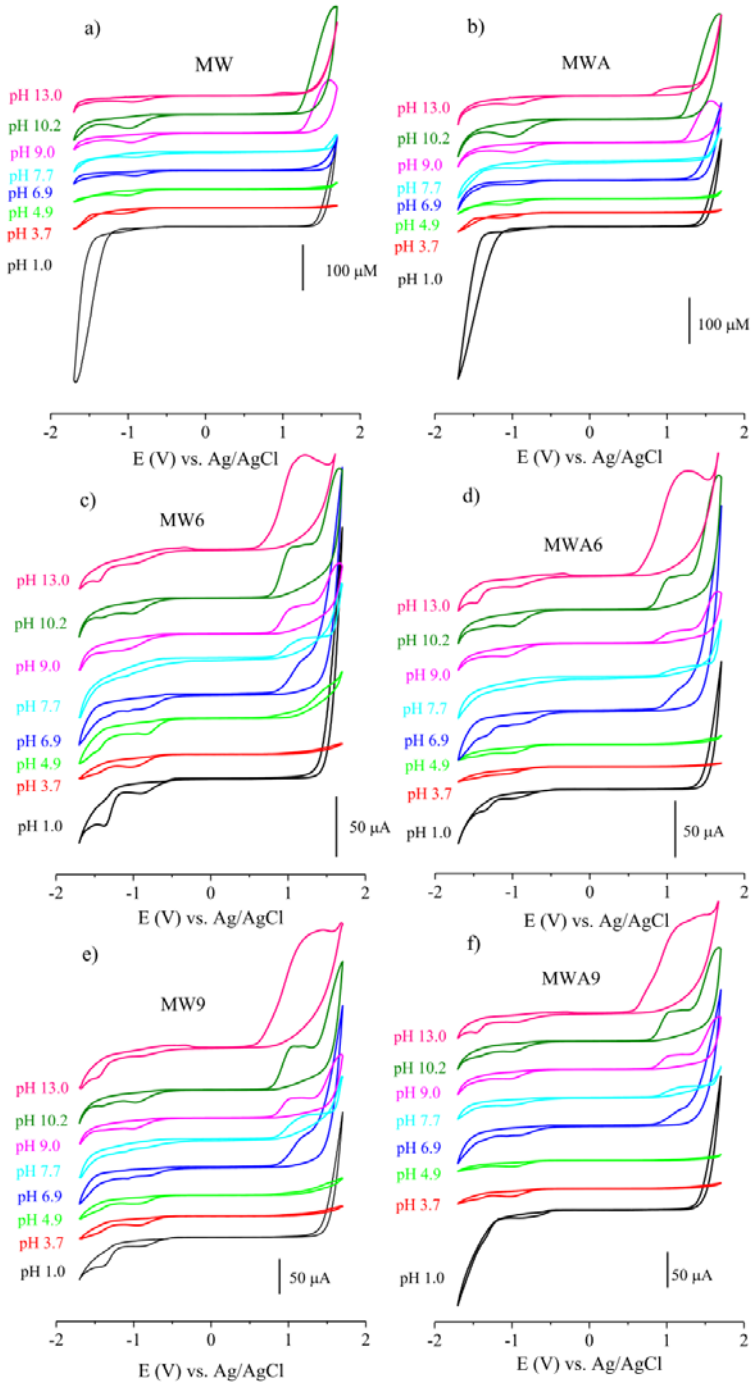

Fig. 3. Cyclic voltammograms recorded at different pH of electrolyte at scan rate of 100 mVs^{-1}.

Electrochemical response of untreated and acid activated clay in corresponding electrolytes was similar. Evolution of oxygen and hydrogen occurred at the margins of employed potential region. Anodic plateau at the foot of oxygen evolution can be seen at voltammograms recorded at pH = 13.0. At pH = 9.0 and pH = 10.2 this process was overlapped with process of oxygen evolution. Possible origin of this wave is formation of oxides on the surface of clay particles. At the potential prior hydrogen evolution cathodic

peak can be seen at all recorded cyclic voltammograms. The peak current of this peak depended on the pH of used electrolyte, but was unaffected by the presence or absence of dissolved oxygen (not shown). The peak was probably consequence of reduction of oxygen species formed in forward sweep.

Two regions of interest are oxidation of nicotine at positive potentials and reduction of nicotine or product of nicotine oxidation at negative potentials. The peak current and peak potential of nicotine oxidation in function of pH of electrolyte are presented in Fig. 4. The response of all investigated clay samples with adsorbed nicotine was similar in corresponding pH. Having in mind differences in the amount of adsorbed nicotine – q_e (Table III) on these four samples this result seems to indicate that only nicotine adsorbed at the specific sites was electroactive. The highest oxidation current response was observed for nicotine adsorbed at untreated clay at pH=9. The current of nicotine oxidation adsorbed on acid activated clay increased with the increase of q_e.

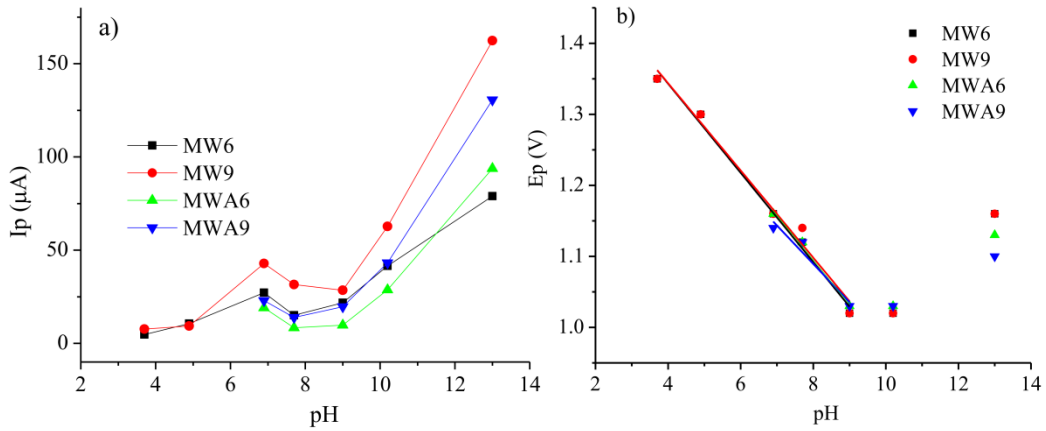

Fig. 4. Effect of the pH on the nicotine peak current (a) and peak potential (b) in different supporting electrolytes.

The oxidation of nicotine adsorbed on untreated clay sample was visible from pH = 3.7. The current response of nicotine adsorbed at acid activated clay sample could be discerned from pH=6.9. The pH dependent electrochemical behavior of each investigated sample followed the same trend regardless of clay treatment or pH at which adsorption was performed. The increase of pH beyond 9 led to the increase of current response. Peak potential showed linear dependence on pH in pH range from 3.7 to 9.0, with slopes of 62.8, 61.4, 62.6 and 54.0 $mVdec^{-1}$ for MW6, MW9, MWA6 and MWA9, respectively. The obtained slopes are close to the value of 59 $mVdec^{-1}$ expected for equal number of protons and electrons involved in the reaction and are in agreement with literature [27, 28]. In the pH region 9.0-10.2 peak potential was independent on pH, while at pH 13 peak potential shifted toward more positive values. The results are in accordance with literature data suggesting that oxidation of nicotine occurs on the nitrogen in pyrrolidine ring [27, 28]. The lack of difference in electrochemical response of monoprotonated and molecular form of nicotine indicated that process of protonization/deprotonization occurred prior to electrochemical oxidation/reduction.

The nicotine reduction process was best resolved at pH = 1. In order to be able to better present the similarities and distinctions for pH=1, voltammograms already presents in Figs. 3c-f are joined together and presented in Fig. 5a. The inserted picture represents the CV of samples without nicotine (already given in Fig 3a-b). Besides, the enlarged part of CV in potential range -1.65 V to -1.25 V is given in Fig. 5b.

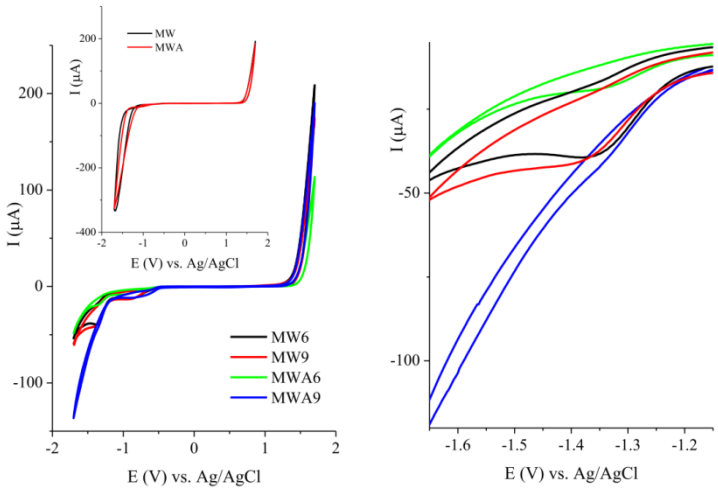

Fig. 5. a) Cyclic voltammograms recorded at MW6, MW9, MWA6 and MWA9 in 0.1 M HCl at 100 mVs^{-1}, inserted picture CV recorded at MW and MWA under the same conditions; b) enlarged parted of Fig. 4a in potential range -1.65 V to -1.25 V.

Nicotine reduction peak visible at potential of -1.35 V is in accordance with literature data [29, 30]. Although the acid treatment causes changes in the surface charges and groups, the voltammograms of untreated and acid activated montmorillonite in 0.1 M HCl were not distinguishable (inset of Fig. 5). The absence of difference between MW and MWA in hydrogen evolution region confirms again that intercalated protons were not involved in the electrochemical response of clay-based electrodes. Reduction of nicotine adsorbed at untreated clay gave almost same current response, regardless of pH of adsorption. On the other hand, reduction of nicotine adsorbed on acid treated clay depended greatly on pH of adsorption. The hydrogen evolution process was completely suppressed on all samples except for MWA9.

There are several ways that nicotine can be adsorbed on the clay. The investigation of nicotine adsorption on clay showed that nicotine can be absorbed through [30]: (i) donation of proton to nicotine by clay; (ii) interaction of lone electron pairs of nitrogen in nicotine with aluminum in clay acting as electron acceptor; (iii) interaction of weakly basic nicotine with weakly acidic hydroxyls; (iv) electrostatic interaction at certain pH values and (v) through hydrogen bond between nitrogen on nicotine and hydroxyl groups of clay.

Our previously published FTIR spectra [12] showed that adsorption of nicotine on untreated clay proceeded mostly through pyrrolidine ring, while formation of hydrogen bond on pyridine ring was noticed for the acid activated clay. According to the XRD results, nicotine was intercalated in all four samples.

Monoprotonated form and molecular form of nicotine are dominant species at pH values at which adsorption was performed [32]. Adsorption of nicotine at pH 6 enabled monoprotonated form to be intercalated as cation in interlamellar space in MW. Similar process can be expected to proceed for MW_A as well, however in lower degree. Kooli *et al.* [33, 34] have investigated intercalation of organic compounds in acid activated clay and found out that cetyltrimethylammonium cations can be intercalated in acid activated clay, but the extent of the intercalation decreased with the extent of acid activation.

Charge sites in clay minerals, including montmorillonite, can be pH dependent or structural sites that are pH independent. Structural sites are the result of isomorphic substitution in clay sheets and their charge remains independent of pH of electrolyte. pH dependent sites originate from terminal under-coordinated OH groups and their sign depend on the pH value of the electrolyte [9]. The surface group at the edges of clay particles change

their charge with pH. According to Kriaa et. al. [35] the two successive protonations and two successive deprotonations occur at the montmorillonite surface. $>AlOH_2^+$ deprotonates to give >AlOH at pH 4-5, followed by deprotonation of $>SiOH_2^+$ to >SiOH at pH 5−8. Deprotonation of >SiOH to $>SiO^-$ occurs at pH≈ 8, while second deprotonation of >AlOH to $>AlO^-$ occurs above pH≈ 10. The number and distribution of surface groups changed with acid activation. Acid treatment of clay causes several changes: interlamellar counter cations are replaced by protons, partial dissolution of smectite layers occurs depending on the initial clay composition, the number of stronger acidic groups (such as $>Al_2\text{-}OH_2^+$, $>Al\text{-}OH_2^+$ and $>Si\text{-}OH_2^+$ decreased [36], while the number of weakly acidic surface groups (such as Al-OH, Si-OH) increased [9].

In order to try to answer which nicotine can be seen by electrochemical method, desorption study at pH = 1 was performed for 30 minutes for all investigated samples (Table II). This desorption time was selected in order to synchronize time scale of desorption with time scale of electrochemical measurements.

Tab. III Results of adsorption-desorption study of nicotine onto selected clay samples.

Sample	**MW6**	**MWA6**	**MW9**	**MWA9**
q_e (mmol g^{-1})	0.434	0.323	0.382	0.541
Retained amount of nicotine after desorption (mmol g^{-1})	0.118	0.175	0.345	0.170
Retained nicotine after desorption (%)	30.1	57.3	92.1	31.4

Desorption was not completely reversible process of nicotine sorption. Desorption of the intercalated organic species is almost completely inhibited for exchangeable cation containing smectites [37]. The amount of nicotine that was retained represents the sum of the amount intercalated in the smectite structure and the amount adsorbed at the clay edges of the clay particles.

According to literature data [38,39] interlayer adsorbed species do not contribute to charge transport. Furthermore, complexes adsorbed at the face surfaces of clay particles in amounts less than or equal to the CEC could be electroactive only in the presence of charge shuttle [40]. It is considered that species adsorbed mostly on the edge sites give rise to the electroactivity of clay-modified electrodes. However, Villemure and Bard [41] as well as King *et al.* [42] considered that all electrostatically bound cations were electrochemically inactive. Investigating the adsorption of enantiomers on clay, Villemure and Bard [43] came to the conclusion that the presence of defects in the films gives rise to the electroactivity of preadsorbed species on the clay-based electrodes. However, only defects that provide the pathway for the electron to the conductive substrate led to the electroactivity.

Literature data on nicotine electroreduction mechanism are very vague. It is possible to make some conclusions based on analogy with available pyridine electroreduction data. The cathodic wave seen at potential around -1.5 V was ascribed to the reduction of hydrogen ion [44]. It was noticed that presence of pyridine in solution affected the current of the wave. The height of the catalytic hydrogen wave is proportional to the concentration of hydrogen ions, concentration of pyridine and the capacity of buffer. The role of the buffer is to regenerate the active cationic form of the pyridine.

Based on analogy, cathodic wave obtained for investigated nicotine-clay samples can be ascribed to the cathodic hydrogen reduction. The direct correlation between wave current intensity and the amount of retained nicotine cannot be established. The ability of pyridine ring in adsorbed nicotine to act as catalyst in this process probably depends on possibility of formation of active forms.

Further insight on investigated systems can be obtained by discussion on hydrogen evolution process. The untreated samples MW6 and MW9 showed similar behavior. On the

other hand, the behavior of acid treated based electrodes depended on the pH of the adsorption. Acid treatment introduces pronounced heterogeneity of layer charge distribution in smectite and favors weak acid sites [9]. Monoprotonated form of nicotine was probably strongly adsorbed at weak acid sites at MWA6 through pyridine nitrogen, leading to the blockage of sites that led to annulling of hydrogen evolution process. At the same time, the occupancy of lone pair on pyridine nitrogen might inhibit its ability to act as catalyst in hydrogen ion reduction process. Molecular nicotine was most likely adsorbed at MWA9 through interaction of pyrrolidine nitrogen lone electron pair with clay sites. The actual geometry of adsorption site and conformation of nicotine can additionally influence the preferential nitrogen involved in interaction with clay.

The obtained results indicated that the most pronounced electrochemical response was not obtained for the sample with the highest amount of retained nicotine. Probably the electrochemical response is related dominantly with non-intercalated nicotine with free pyridine nitrogen after established nicotine-clay interaction.

4. Conclusion

Nicotine was adsorbed on untreated and acid activated montmorillonite clay in monoprotonated (at pH = 6) and molecular form (at pH = 9.26). XRD analysis showed that nicotine was intercalated into interlamellar space of montmorillonite in a form of monolayer. The nicotine-modified untreated clay used as paste electrode showed enhanced electrochemical response toward ferrocyanide probe in comparison to electrode based on clay without nicotine. On the other hand, adsorbed nicotine on acid activate clay resulted in lower electrode activity.

The pH dependent electrochemical nicotine oxidation at each of investigated samples followed the same trend regardless of clay treatment or pH at which adsorption was performed. For all samples, nicotine oxidation peak potential showed linear dependence on pH in pH range from 3.7 to 9.0, with slopes close to the value of 59 $mVdec^{-1}$ expected for equal number of protons and electrons involved in the reaction.

The nicotine reduction process was best resolved at pH = 1 at potential around -1.35 V, while the following cathodic wave observed at potential around -1.5 V was ascribed to the cathodic hydrogen reduction. The direct correlation between wave current intensity and the amount of retained nicotine was not found.

The free pyridine nitrogen has a great potential for the fabrication of electrochemical sensor. Future research will involve investigation of the electrochemical reactivity of the nicotine-clay modified electrode toward appropriate analytes.

Acknowledgments

This work was supported by the Ministry of Education, Science and Technological Development of the Republic of Serbia (Contract No. 451-03-9/2021-14/200026).

5. References

1. M. Kokunešoski, M. Stanković, M. Vuković, J. Majstorović, Đ. Šaponjić, S. Ilić, A. Šaponjić, Sci. Sinter. 52 (2020) 339.
2. A. Adauto, M. R. Sun-Kou, Environ. Nanotechnol. Monit. Manag., 15 (2021) 100476.
3. R. Yang, J. Cai, H. Yang, Sci. Total Environ., 773 (2021) 145661.

4. A. Hamza, I. A. Hussein, M. J. Al-Marri, M. Mahmoud, R. Shawabkeh, Int. J. Greenh. Gas Control.106 (2021) 103286.
5. I. K. Tonle, E. Ngameni, F. M. M. Tchieno, A. Walcarius, J. Solid State Electrochem., 19 (2015) 1949.
6. M. O. Miranda, B. C. Viana, L. M. Honório, P. Trigueiro, M. G. Fonseca, F. Franco, J. A. Osajima, E. C. Silva-Filho, Minerals, 10 (2020) 132.
7. M. Paramasivam, G. Anandhan, Bull. Chem. Soc. Jpn., 78 (2005) 1783.
8. T. Novaković, N. Abazović, T. Savić, M. Čomor, Z. Mojović, Sci. Sinter., 52 (2020) 359.
9. F. Bergaya, G. Lagaly, Handbook of clay science, developments in clay science, Amsterdam: Elsevier, 2013.
10. L. B. de Paiva, A. R. Morales, F. R. Valenzuela-Díaz, Appl. Clay Sci., 42 (2008) 8.
11. C. Mousty, Appl. Clay Sci. 27 (2004) 159.
12. I. Ilić, N. Jović-Jovičić, P. Banković, Z. Mojović, D. Lončarević, I. Gržetić, A. Milutinović-Nikolić, Sci. Sinter., 51 (2019) 93.
13. K. R. Olson, Poisoning, Drug Overdose, Mac Graw-Hill, New York, 2006.
14. J. Seckar, M. Stavanja, P. Harp, Y. Yi, C. Garner, J. Doi, Environ. Toxicol. Chem., 27 (2008) 1505.
15. Water Sentinel Online Water Quality, Monitoring as an Indicator of Drinking Water Contamination, EPA 817-D-05-002, US Environmental Protection Agency, 2005 (verified May 2021).
16. Clay Minerals Society, Source Clay Physical/Chemical Data. http://www.clays.org/Sourceclays.html (verified May 2021).
17. A. R. Mermut, A. F. Cano, Clays Clay Miner., 49 (2001) 374.
18. Z. Vuković, A. Milutinović-Nikolić, Lj. Rožić, A. Rosić, Z. Nedić, D. Jovanović, Clays Clay Miner., 54 (2006) 697.
19. International Center for Diffraction Data, Joint Committee on Powder Diffraction Standards JCPDS, 1990, Swarthmore, USA.
20. D. M. R. Moore, C. Reynolds, X-Ray Difraction and the Identification and Analysis of Clay Minerals, OxfordUniversity Press, New York, 1997.
21. E. P. Rebitski, P. Aranda, M. Darder, R. Carraro, E. Ruiz-Hitzky, Dalton Trans., 47 (2018) 3185.
22. C. Ruiz-García, J. Pérez-Carvajal, A. Berenguer-Murcia, M. Darder, P. Aranda, D. Cazorla-Amorós, E. Ruiz-Hitzky, Phys. Chem. Chem. Phys., 15 (2013) 18635.
23. P. Falaras, F. Lezou, P. Pomonis, A. Ladavos, J. Electroanal. Chem. 486 (2000) 156.
24. I. K. Tonle, E. Ngameni, A. Walcarius, Electrochim. Acta 49 (2004) 3435.
25. Z. Navrátilová, M. Mucha, J. Solid State. Electrochem. 19 (2015) 2013.
26. N. Jović-Jovičić, M. Mojović, D. Stanković, B. Nedić-Vasiljević, A. Milutinović-Nikolić, P. Banković, Z. Mojović, Electrochim. Acta 296 (2019) 387.
27. H. B. Suffredini, M. C. Santos, D. De Souza, L. Codognoto, P. Homem-de-Mello, K. M. Honório, A. B. F. da Silva, S. A. S. Machado, L. A. Avaca, Anal. Lett., 38 (2005) 1587.
28. A. Levent, Y. Yardim, Z. Senturk, Electrochim. Acta 55 (2009) 190.
29. H. Xiong, Y.Zhao, P. Liu, X. Zhang, S. Wang, Microchim. Acta, 168 (2010) 31.
30. Y. Jing, B. Yu, P. Li, B. Xiong, Y. Cheng, Y. Li, C. Li, X. Xiao, M Chen, L Chen, Y. Zhang, M. Zhao, C. Cheng, Sci. Rep. 7 (2017) 14332.
31. J. P. Singhal, R.P. Singh, Studies on the adsorption of nicotine on kaolinites, Soil Sci. Plant Nutr., 22 (1979) 35.
32. E.W. Willems, B. Rambali, W. Vieeming, A. Opperhuizen, J.G.C. van Amsterdam, Food Chem. Toxicol., 44 (2006) 678.
33. F. Kooli, Y. Z. Khimyak, S. F. Alshahateet, F. Chen, Langmuir, 21 (2005) 8717.
34. F. Kooli, J. Chem. 1155 (2015) 919636.

35. A. Kriaa, N. Hamdi, E. Srasra, Russ. J. Electrochem., 43 (2007) 167.
36. G. Jozefaciuk, Clays Clay Miner., 50 (2002) 647.
37. W. Zhang, Y. Ding, S. A. Boyd, B. J. Teppen, H. Li, Chemosphere, 81 (2010) 954.
38. W. Rudzinski, A. J. Bard, J. Electroanal. Chem., 199 (1986) 323.
39. C. M. Castro-Acuna, F.-R. F. Fan, A. J. Bard, J. ElectroanaL Chem., 234 (1987) 347.
40. A. Fitch, Clays Clay Miner., 38 (1990) 391.
41. G. Villemure, A.J. Bard, J. Electroanal. Chem., 282 (1990) 107.
42. R. D. King, D. G. Nocera, T. J. Pinnavaia, J. Electroanal. Chem., 236 (1987) 43.
43. G. Villemure, A. J. Bard, J. Electroanal. Chem., 283 (1990) 403.
44. G. Dryhurst, Pyridine and Pyridine Nucleotides in Electrochemistry of Biological Molecules, Academic Press, New York, 1977.

Сажетак: *Глина са високим садржајем монморијонита је кисело активирана. Извршена је адсорпција никотина из воденог раствора на полазној и кисело-активираној глини на pH=6 или pH=9,26 (неподешен pH раствора). На основу резултата XRD анализе утврђено је да је након адсорпције никотина међураванско растојање 001 равни монморијонита 1,38 nm, без обзира на то да ли је глина активирана или не, као и на којој pH је адсорпција вршена. Добијене вредности за међураванско растојање указују да је никотин уграђен у облику монослоја. Полазна и кисело-активирана глина, са и без никотина коришћене су за модификацију карбон-паста електроде да би се испитала електрохемијска својства. Циклична волтаматрија и електрохемијска импедансна спектроскопија су коришћене да би се испитао електрохемијски одговор према фероцијанидној проби глином-модификованих електрода. Полазна никотином-модификована глина коришћена као паста-електрода показала је бољи електрохемијски одговор према фероцијанидној проби у односу на електроду на бази глине без никотина. Насупрот томе, никотин адсорбован на кисело-активираној глини довео је до смањења електродне активности. Електрохемијски одговор адсорбованог никотина испитиван је на различитим pH вредностима раствора. Оксидација никотина је код свих испитиваних узорка имала исти тренд, без обзира на киселу модификацију и/или pH вредност на којој је вршена адсорпција. Код свих узорака, потенцијал на којем се налази пик оксидације никотина показује линеарну зависност од pH у интервалу pH од 3,7 до 9,0, са нагибом приближно 59 mVdec^{-1} што одговара реакцији у којој је укључен једнак број протона и електрона. Процес редукције никотина најбоље се уочава на pH = 1 на потенцијалу око -1,35 V, док је катодни талас који следи на потенцијалу око -1,5 V приписан катодној редукцији водоника. На механизам електрохемијске оксидације нису утицали ни pH адсорпције, као ни форма никотина присутна на тој pH вредности. Количина адсорбованог никотина није утицала на електрохемијску активност указујући да је само мала количина адсорбованог никотина учествовала у електрохемијском одговору.*

Кључне речи*: никотин, монморијонит, циклична волтаметрија, електрохемијска импедансна спектроскопија, фероцијанидна проба.*